ЯДЕРНА ФІЗИКА
NUCLEAR PHYSICS

УДК 539.142 https://doi.org/10.15407/jnpae2023.04.316

A. H. Ali[1,2,*]

[1] *College of Medicine, University of Fallujah, Fallujah, Iraq*
[2] *Biotechnology and Environmental Center, University of Fallujah, Anbar, Iraq*

*Corresponding author: dr.ahmedphysics@uofallujah.edu.iq

A COMPARISON BETWEEN THEORETICAL RESULTS AND EXPERIMENTAL DATA OF TRANSITION PROBABILITY *B*(*E*2), DEFORMATION PARAMETER, AND INTRINSIC QUADRUPOLE MOMENTS FOR DIFFERENT NUCLEI WITH THE MASS NUMBER A = 44

A comparison has been made between theoretical results and the experimental data for different nuclei (even-even) that possess the same mass number A = 44 and which have close values of the experimental deformation parameter such as $_{16}S^{44}$, $_{18}Ar^{44}$, $_{20}Ca^{44}$ and $_{22}Ti^{44}$. The core-polarization effects and model space were adopted through the inclusion of effective charges. Transition probability *B*(*E*2), theoretical deformation parameters, and theoretical intrinsic quadrupole moments were calculated using two different interactions for each case, the first case the *hasp* interaction for nuclei in the *sd* shell, and the *fpd6* interaction for nuclei in the *fp* shell, the second case the *vpnp* interaction for nuclei in the *sd* shell, and the *kb3* interaction for nuclei in the *fp* shell, as well as adopted to different effective charges, such as Bohr and Mottelson effective charges, standard effective charges, and the effective charges from program NuShellX. The theoretical results of the transition probability *B*(*E*2), deformations parameters, and intrinsic quadrupole moments were compared and found to be close to the experimental values for these nuclei.

Keywords: comparison, deformation parameter, effective charges, nuclei, intrinsic quadrupole moments.

1. Introduction

The deformation parameters of nuclei are vital to an understanding of their shapes, namely whether they are oblate or prolate. The shape transition can be calculated from the quadrupole deformation [1]. Calculations of the deformation parameter are dependent on the effective interactions. The *sd* shell is very interesting theoretically because it is very suitable for studying nuclear models. Studying cores in the *sd* shell can lead to a better understanding between the macroscopic (collective) description and the microscopic description (shell model) [2]. Where nuclei in the *sd* shell have an inert nucleus ^{16}O and valence nucleons are distributed in the *sd* shell ($1d_{5/2}$, $2s_{1/2}$, and $1d_{3/2}$) [3, 4]. The interaction for the *sd* model space was studied in [5].

A nucleon-nucleon-free interaction can be used to derive the effective interaction, where these interactions are adopted for the *fp* shell [6, 7]. In cases where there are a large number of valence nucleons, e.g., ^{48}Ca and ^{56}Ni, these interactions have been found to fail [7, 8]. Particularly in ^{56}Ni, it has been predicted that the ground state will be largely deformed when calculating with the full *fp* shell; conversely, it is known to have a double magic structure. The four single-particle energies of the 195 two-body matrix elements and the *fp* shell, have been determined from the study of similar approaches by Richter et al. [9]. These solutions, which depended on a semiempirical interaction were obtained using a core polarization correction and the single-boson exchange potential [9]. Calculations of the shell model in the *fp* shell, when orbits are full, were performed for atoms of equal mass number (isobar), as studied by A. Poves et al. [10]. The interactions for the *fp* model space, *fpd6* [9], and *kb3* [10] were studied and their behavior at the $N = 28$ and $Z = 28$ closures was investigated. The effective charges were determined in the *fp* shell by calculations. Calculations of the shell model which include a diagonalization matrix were carried out for several effective interactions, namely *fpd6* [9] and *kb3* [10]. The reduced quadrupole deformation parameter can be denoted by the symbol β_2 which can be calculated from the transition rate (reduced electric transition probability) *B*(*E*2). The quadrupole-deformed nuclei were classified according to their intrinsic electric quadrupole moment Q_0, that is, as oblate when Q_0 is greater than zero or prolate when Q_0 is less than zero and, as spherical nuclei when Q_0 is equal to zero [11]. Novoselsky et al. [12] studied two interactions, *fpm13* and *fpd6*, in terms of giving good, suitable energy levels for nuclei in the lower part of the *fp* shell, where the mass factors, $\left(\frac{A}{42}\right)^{-0.35}$, (where A denotes the number of nucleons) was used [9].

The code for NuShellX@MSU is written by Brown [13] and is achieved via model spaces and Hamiltonian data with regard to generating inputs for NU-SH. The code also transforms the NU-SH files (output) into Tables and Figures, as well as gamma and beta decays, and energy levels [13]. The deformation parameter was calculated using two different interactions, *kb3*, and *fpd6*, and various effective charges, B-M, ST, and NU-SH.

Calculating the quadrilateral deformation parameters is important to study the deformations of nuclei. The deformation parameters can be calculated from the probability of transitions *B*(*E*2) and through the intrinsic quadrupole moment Q_0. The theoretical results obtained were compared with the experimental results. From the calculated theoretical values of *B*(*E*2) the theoretical deformation parameters were calculated which were compared with the practical values of almost equal deformation parameters for the nuclei under study.

2. Theory

The charge distribution can be defined by the electric transition operator, O (*E*2) as:

$$\hat{O}(EJ)=\sum_{k=1}^{A} e(k) r^{J}(k) Y_{J}\left(\vec{r}(k)\right), \qquad (1)$$

where number of charges k in nucleon by $e(k)$, $e(k) = e$ for a proton and $e(k) = 0$ for a neutron. The $J_f \left\| \hat{O}_J \right\| J_i$ reduced matrix element defined as [11]

$$\left\langle J_f \left\| \hat{O}_J \right\| J_i \right\rangle = \sum_{jj'} OBDM\left(J_i, J_f, J, j, j'\right) \left\langle j' \left\| \hat{O}_J \right\| j \right\rangle \qquad (2)$$

with j, j' representing initial and final single-particle states, single-particle matrix elements are represented by $\left\langle j' \left\| \hat{O}_J \right\| j \right\rangle$, and the one body density matrix represented by one-body density matrices (OBDM). The equation represents to matrix elements of model space [11]

$$\left\langle J_f \left\| \hat{O}_J \right\| J_i \right\rangle = \sum_{t_z} e^{eff}\left(t_z\right) \left\langle J_f \left\| \hat{O}_J \right\| J_i \right\rangle_{iMS}, \qquad (3)$$

where e^{eff} denote the effective charges of protons and neutrons that are active in the restricted model space.

An expression for the effective charges to explicitly include neutron excess is formulated as [14, 15]:

$$e^{eff}\left(t_z\right) = e\left(t_z\right) + e\delta e\left(t_z\right),$$

$$\delta e\left(t_z\right) = Z/A - 0.32\left(N-Z\right)/$$

$$/A - 2t_z\left[0.32 - 0.3\left(N-Z\right)/A\right]. \qquad (4)$$

B(*E*2) can be defined through the transition from the initial state J_i to the finial state J_f [16]:

$$B\left(EJ\right) = \frac{\left\langle J_f \left\| \hat{O}_J \right\| J_i \right\rangle^2}{2J_i + 1}. \qquad (5)$$

The quadrupole deformation parameter (β_2) can be calculated from the reduced electric quadrupole transition probability, *B*(*E*2)↑, according to [1, 16]:

$$\beta_2 = \left(\frac{4\pi}{3ZR_0^2}\right)\left[B\left(E_2\right)\uparrow \frac{e^2 fm^4}{e^2}\right]^{1/2}, \qquad (6)$$

where $R_0 = 1.2\ A^{1/3}\ fm$, Z represents the atomic number, while the intrinsic electric quadrupole moment Q_0 can be calculated by [17, 18]:

$$Q_0 = \sqrt{\frac{16\pi}{5}}\left[B\left(E2\right)\right]^{1/2}. \qquad (7)$$

The deformation parameters (β_2) for the lighter nuclei are somewhat large [15], while the deformation parameters of heavy nuclei are smaller than zero where they are prolate in shape and are strongly deformed.

3. Results and discussion

The OBDM were calculated using the program NuShellX@MSU [13], which adopted four interactions, namely *hasp* interaction [5] for the s*d* model space and *fpd6* interaction [9] for the *fp* model space, while *vpnp* interaction [19] was adopted for the *sd* model space and *kb3* interaction [10] for the *fp* model space. The core-polarization effects and model space were adopted through the inclusion of effective charges. Transition probability *B*(*E*2), theoretical deformation parameters, theoretical intrinsic quadrupole moments, and deformations parameters were calculated using two different interactions for each case, the first case the *hasp* interaction for nuclei in the *sd* shell, and the *fpd6* interaction for nuclei in the *fp* shell, the second case the *vpnp* interaction for nuclei in the *sd* shell, and the *kb3* interaction for nuclei in the *fp* shell. Three sets of effective charges were adopted, with Bohr - Mottelson (B-M) effective charges calculated [15] according to Eq. (4), the results of which are tabulated in Table 1 for all nuclei considered in the present work, where the standard (ST) effective charges are e_p = 1.36*e*

and e_n = 0.45e [16]. Finally, the effective charges NU-SH are e_p= 1.5e and e_n = 0.5e which are taken from program NU-SH [13].

3.1. Transition rate $B(E2)$

Theoretical transition rates $B_{\text{Theo.1}}(E2)$ [17] were calculated for the nuclei $_{16}S^{44}$, $_{18}Ar^{44}$, $_{20}Ca^{44}$, and $_{22}Ti^{44}$ using *hasp* [5] and *fpd6* interactions [9]. The $B_{\text{Theo.1}}(E2)$ for $_{16}$S with the B-M effective charges was 231 e^2fm^4, the $B_{\text{Theo.1}}(E2)$ with the ST effective charges was 264 e^2fm^4, and the $B_{\text{Theo.1}}(E2)$ for $_{16}$S with the NU-SH effective charges was 324 e^2fm^4, the results of the $B_{\text{Theo.1}}(E2)$ with the NU-SH effective charges were found to be the closest to the experimental values [17, 20]. The $B_{\text{Theo.1}}(E2)$ for $_{18}$Ar with the B-M effective charges was 616 e^2fm^4, the $B_{\text{Theo.1}}(E2)$ for $_{18}$Ar with the ST effective charges was 650 e^2fm^4, and the $B_{\text{Theo.1}}(E2)$ for $_{18}$Ar with the NU-SH effective charges was 794 e^2fm^4, the calculations of the $B_{\text{Theo.1}}(E2)$ with any of the effective charges underestimate the experimental values [20]. The $B_{\text{Theo.1}}(E2)$ for $_{20}$Ca with the B-M effective charges was 144 e^2fm^4, the $B_{\text{Theo.1}}(E2)$ for the $_{20}$Ca with the ST effective charges was 56 e^2fm^4, and the $B_{\text{Theo.1}}(E2)$ for the $_{20}$Ca with the NU-SH effective charges was 70 e^2fm^4. The calculations of the $B_{\text{Theo.1}}(E2)$ with any of the effective charges overestimate the experimental values [20]. Calculations of $B_{\text{Theo.1}}(E2)$ for $_{22}$Ti with the B-M and the NU-SH effective charges were 698 e^2fm^4 close to the experimental values [20]. While calculations of $B_{\text{Theo.1}}(E2)$ for $_{22}$Ti with the ST effective charges was 572 e^2fm^4, it underestimated the experimental values [20], as in Table 1 and Fig. 1.

Table 1. **The $B_{\text{Theo.1}}(E2)$ were calculated for certain nuclei $_{16}S^{44}$, $_{18}Ar^{44}$, $_{20}Ca^{44}$, and $_{22}Ti^{44}$ with *hasp* [5] and *fpd6* interactions [9], and compared with the corresponding experimental values [17, 20]**

Z, N A = 44	$(E_x)_{\text{Exp}}$, keV	$(E_x)_{\text{Theo}}$, keV	e_p, e_n	$B(E2)_{\text{Theo}}$, e^2fm^4 B-M	$B(E2)_{\text{Theo}}$, e^2fm^4 ST	$B(E2)_{\text{Theo}}$, e^2fm^4 NU-SH	$B(E2)_{\text{Exp}}$, e^2fm^4
16, 28	1315	1870	1.04, 0.51	231	264	324	310 ± 90
18, 26	1144	2324	1.09, 0.62	616	650	794	345 ± 41
20, 24	1157	1619	1.13, 0.72	144	56	70	470 ± 20
22, 22	1082	1300	1.18, 0.82	698	572	698	650 ± 160

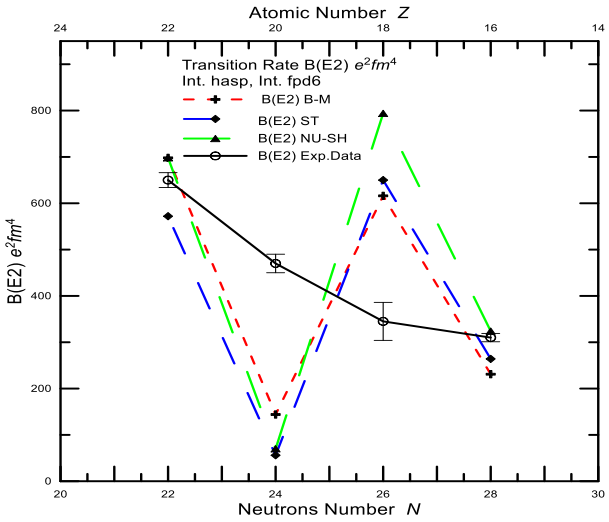

Fig. 1. $B_{\text{Theo.1}}(E2)$ values were calculated for certain nuclei $_{16}S^{44}$, $_{18}Ar^{44}$, $_{20}Ca^{44}$, and $_{22}Ti^{44}$ when considering *hasp* [5] and *fpd6* interactions [9]. Calculated values are compared with experimental ones [17, 20]. (See color Figure on the journal website.)

Theoretical values for transition rate $B_{\text{Theo.2}}(E2)$ values were calculated for certain nuclei $_{16}S^{44}$, $_{18}Ar^{44}$, $_{20}Ca^{44}$, and $_{22}Ti^{44}$ using interactions determined via *vpnp* [19] for the *sd* model space and *kb3* [10] for the *fp* model space. Theoretical results were compared with the experimental values [17, 20], as shown in Table 2 and Fig. 2. The $B_{\text{Theo.2}}(E2)$ for $_{16}$S was calculated using the B-M effective charges 219 e^2fm^4, using the ST effective charges 247 e^2fm^4, and using the NU-SH effective charges 303 e^2fm^4. Theoretical calculations of transition rate $B_{\text{Theo.2}}(E2)$ with the NU-SH effective charges agreed with the experimental values [20]. $B_{\text{Theo.2}}(E2)$ values were calculated for $_{18}$Ar with the B-M effective charges 406 e^2fm^4, the ST effective charges 388 e^2fm^4, and the NU-SH effective charges 474 e^2fm^4, which were found to be very close to the experimental values [20], while calculations of $B_{\text{Theo.2}}(E2)$ with the B-M and the ST effective charges are overestimated comparing to the experimental values [20].

Table 2. **Theoretical values of transition rate $B_{\text{Theo.2}}(E2)$ values were calculated for certain nuclei $_{16}S^{44}$, $_{18}Ar^{44}$, $_{20}Ca^{44}$, and $_{22}Ti^{44}$ with *vpnp* [19] and *kb3* interactions [10], and were compared with the experimental values [17, 20]**

Z, N A = 44	$(E_x)_{\text{Exp}}$, keV	$(E_x)_{\text{Theo}}$, keV	e_p, e_n	$B(E2)_{\text{Theo}}$, e^2fm^4 B-M	$B(E2)_{\text{Theo}}$, e^2fm^4 ST	$B(E2)_{\text{Theo}}$, e^2fm^4 NU-SH	$B(E2)_{\text{Exp}}$, e^2fm^4
16, 28	1315	1870	1.04, 0.51	219	247	303	310 ± 90
18, 26	1144	1786	1.09, 0.62	406	388	474	345 ± 41
20, 24	1157	1278	1.13, 0.72	115.7	45.4	56	470 ± 20
22, 22	1082	1321	1.18, 0.82	610	494	610	650 ± 160

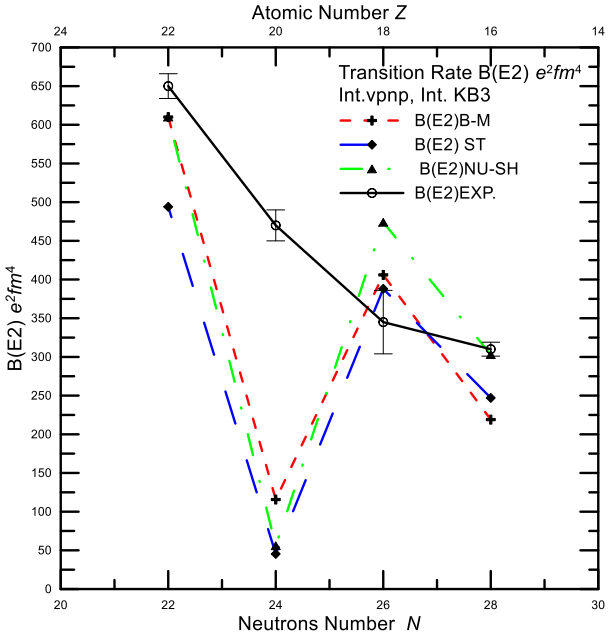

Fig. 2. The $B_{\text{Theo.2}}(E2)$ values were calculated for certain nuclei $_{16}S^{44}$, $_{18}Ar^{44}$, $_{20}Ca^{44}$, and $_{22}Ti^{44}$ with *vpnp* [19] and *kb3* interactions [10], as compared with the experimental values [17, 20]. (See color Figure on the journal website.)

3.2. Deformation parameter

The theoretical deformation parameters were calculated from the theoretical values of $B(E2)$, which were dependent on effective charges, such as the B-M, ST, and NU-SH. The theoretical results for the deformation parameters were compared with experimental values [17, 20]. The theoretical deformation parameters $\beta_{\text{Theo.1}}$ values were calculated from $B_{\text{Theo.1}}(E2)$ values, which were calculated from two interactions, *hasp* for the *sd* shell and *fpd6* for the *fp* shell. The theoretical values of the deformation parameter $\beta_{\text{Theo.1}}$ for the nuclei of Z = 16 and 22 were close to the experimental values, while the $\beta_{\text{Theo.1}}$ for the nucleus of Z = 18 overestimated the experimental values [20]. The $\beta_{\text{Theo.1}}$ for the nucleus of Z = 20, however, underestimated the experimental values [20] (Table 3 and Fig. 3).

Table 3. **Calculations of the theoretical deformation parameter $\beta_{\text{Theo.1}}$ for the nuclei with atomic numbers Z = 16, 18, 20, and 22 with two interactions, *hasp* [5] for the *sd* shell and *fpd6* [9] for the *fp* shell, which adopted values of $B(E2)$ calculated using the B-M [15], ST [16, 21] and NU-SH [13] effective charges. These $\beta_{\text{Theo.1}}$ values were compared with experimental values [17, 20]**

Z, N A = 44	$\beta_{\text{Theo.1}}$ B-M	$\beta_{\text{Theo.1}}$ ST	$\beta_{\text{Theo.1}}$ NU-SH	$\beta_{\text{Exp.}}$
16, 28	0.237	0.221	0.262	0.254 ± 0.038
18, 26	0.321	0.330	0.365	0.240 ± 0.014
20, 24	0.14	0.08	0.09	0.253 ± 0.005
22, 22	0.28	0.253	0.28	0.268 ± 0.034

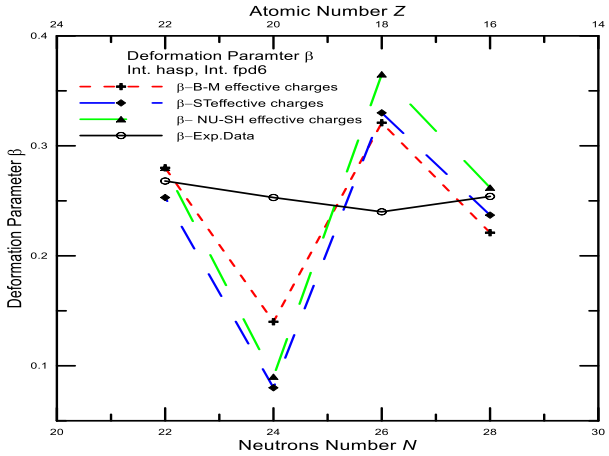

Fig. 3. Calculations of deformation parameter $\beta_{Theo.1}$ for the nuclei with atomic numbers Z = 16, 18, 20, 22 with two interactions, *hapn* [5] and *fpd6* [9], which adopted values of $B_{Theo.1}(E2)$ calculated from B-M [15], ST [16, 21] and NU-SH [9] effective charges. The $\beta_{Theo.1}$ were compared with the experimental values [17, 20]. (See color Figure on the journal website.)

The $\beta_{Theo.2}$ values were calculated using $B_{Theo.2}(E2)$ values which were calculated from two interactions, *vpnp* [19] for the *sd* shell and *kb3* [10] for the *fp* shell. The $\beta_{Theo.2}$ determined for the nuclei of Z = 16, 18, and 22 were close to the experimental values, while the $\beta_{Theo.2}$ of the nucleus of Z = 20 was underestimated comparing to experimental values [17] (Table 4 and Fig. 4).

Table 4. **Calculations of the $\beta_{Theo.2}$ for nuclei with atomic numbers Z = 16, 18, 20, and 22 with two interactions, *vpnp* [19] and *kb3* [10], which adopted values of $B_{Theo.2}(E2)$ calculated using B-M [15], ST [16, 21], and NU-SH [13] effective charges. The $\beta_{Theo.2}$ values were compared with experimental values [17, 20]**

Z, N A = 44	$\beta_{Theo.2}$ B-M	$\beta_{Theo.2}$ ST	$\beta_{Theo.2}$ NU-SH	$\beta_{Exp.}$
16, 28	0.216	0.2293	0.254	0.254 ± 0.038
18, 26	0.26	0.25	0.28	0.240 ± 0.014
20, 24	0.125	0.078	0.08	0.253 ± 0.005
22, 22	0.262	0.235	0.262	0.268 ± 0.034

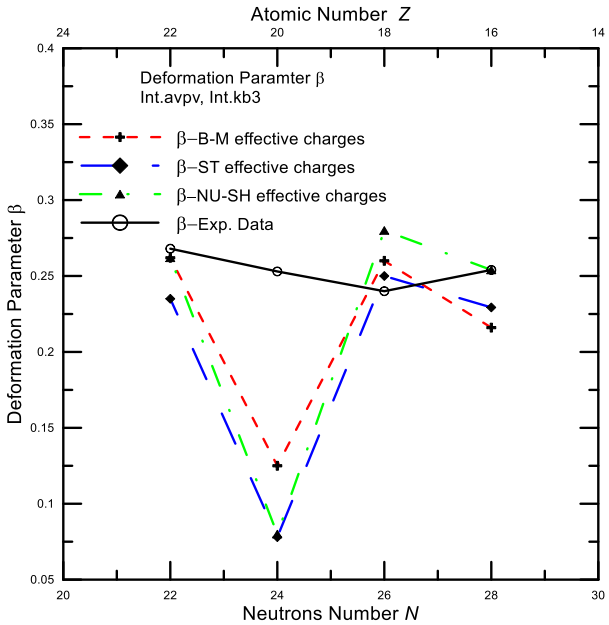

Fig. 4. Calculations of $\beta_{Theo.2}$ for nuclei with atomic numbers Z = 16, 18, 20, and 22 with two interactions, *vpnp* [19] and *kb3* [10], which adopted values of $B_{Theo.2}(E2)$ calculated using the B-M [15], ST [16, 21] and NU-SH [13] effective charges. The results were compared with experimental values [17, 20]. (See color Figure on the journal website.)

3.3. Intrinsic quadrupole moments

Theoretical intrinsic quadrupole moments $Q_{0\text{Theo.1}}\,fm^2$ were calculated for the nuclei A = 44 with atomic numbers Z = 16, 18, 20, and 22 (neutrons numbers N = 28, 26, 24, and 22) with two interactions, *hasp* [5] and *fpd6* [9], which adopted values of $B_{\text{Theo.1}}(E2)$ calculated from effective charges such as B-M [15], ST [16, 21] and NU-SH [13]. The theoretical values of $Q_{0\text{Theo.1}}$ for nuclei of Z = 22 and 16 (N = 22, 28) were close to the experimental values [20], while the $Q_{0\text{Theo.1}}$ for the nucleus of Z = 18 (N = 26) were overestimated comparing to the experimental values [20].

The $Q_{0\text{Theo.1}}$ for the nucleus of Z = 20 (N = 24) was underestimated compared to experimental values [20]. Theoretical intrinsic quadrupole moments were comparing with experimental values [17, 20] (Table 5 and Fig. 5).

Table 5. **Calculations of the intrinsic quadrupole moments $Q_{0\text{Theo.1}}$ for nuclei with atomic numbers Z = 16, 18, 20, and 22 with two interactions, *hasp* [5] and *fpd6* [9], which adopted values of $B_{\text{Theo.1}}(E2)$ calculated from the B-M [15], ST [16, 21], and NU-SH [13] effective charges. The intrinsic quadrupole moments were compared with the experimental values [17, 20]**

Z, N A = 44	$Q_{0\text{Theo.}}$, fm^2 B-M	$Q_{0\text{Theo.}}$, fm^2 ST	$Q_{0\text{Theo.}}$, fm^2 NU-SH	$Q_{0\text{Exp.}}$, fm^2
16, 28	48	51	57	55 ± 8
18, 26	78.6	80.7	89.2	58.8 ± 3.5
20, 24	30.02	23.7	26.5	68.7 ± 1.5
22, 22	83.7	75.8	83.7	80 ± 10

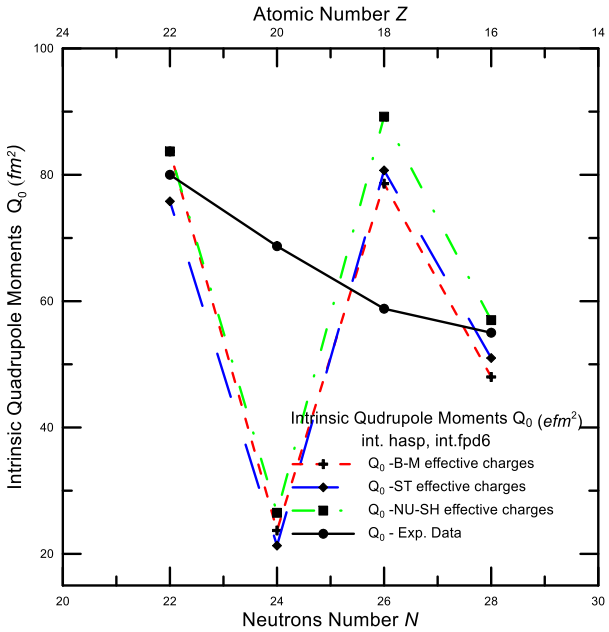

Fig. 5. Calculations of the theoretical intrinsic quadrupole moments $Q_{0\text{Theo.1}}$ for nuclei A = 44 with atomic numbers of Z = 16, 18, 20, and 22 with two interactions, *hasp* [5] and *fpd6* [9], which adopted values of $B_{\text{Theo.1}}(E2)$ calculated using the B-M [15], ST [16, 21], and NU-SH [13] effective charges. The intrinsic quadrupole moments were compared with experimental values [17, 20]. (See color Figure on the journal website.)

The $Q_{0\text{Theo.2}}$ were calculated for nuclei A = 44 with atomic numbers of Z = 16, 18, 20, and 22 (neutrons numbers N = 28, 26, 24, and 22) with two interactions, *vpnp* [19] and *kb3* [10], which adopted values of $B_{\text{Theo.2}}(E2)$ calculated using the B-M [15], ST [16, 21], and NU-SH [13] effective charges. The results were compared with experimental values [17, 20]. The theoretical values of the $Q_{0\text{Theo.2}}$ for nuclei Z = 16, 18, and 22 (N = 22, 26, and 28) were close to the experimental values [20], while the $Q_{0\text{Theo.2}}$ for the nucleus of Z = 20 (N = 24) underestimated them [17, 20] (Table 6 and Fig. 6).

Table 6. **Calculations of the $Q_{0\text{Theo.}2}$ for nuclei with atomic numbers Z = 16, 18, 20, and 22 with two interactions, *vpnp* [19] and *kb3* [10], which adopted values of $B_{\text{Theo.}2}(E2)$ calculated from the B-M [15], ST [16, 21] and NU-SH [13] effective charges. The intrinsic quadrupole moments were compared with experimental values [17, 20]**

Z, N A = 44	$Q_{0\text{Theo.}}$, fm^2 B-M	$Q_{0\text{Theo.}}$, fm^2 ST	$Q_{0\text{Theo.}}$, fm^2 NU-SH	$Q_{0\text{Exp.}}$, fm^2
16, 28	46.9	49.8	55.5	55 ± 8
18, 26	63.8	62.4	69	58.8 ± 3.5
20, 24	34.08	21.3	23.7	68.7 ± 1.5
22, 22	78.2	70.4	78.2	80 ± 10

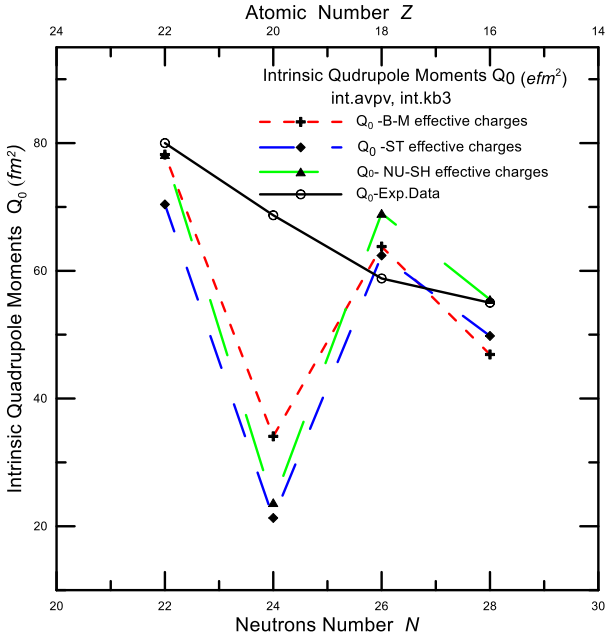

Fig. 6. Calculations of $Q_{0\text{Theo.}2}$ for nuclei A = 44 with atomic numbers Z = 16, 18, 20, and 22 with two interactions, *vpnp* [19] and *kb3* [10], which adopted values of $B_{\text{Theo.}2}(E2)$ calculated from the B-M [15], ST [16, 21], and NU-SH [13] effective charges. The intrinsic quadrupole moments were compared with experimental values [17, 20]. (See color Figure on the journal website.)

4. Conclusion

A theoretical comparison has been made for different even-even nuclei that have the same mass number A = 44, namely $_{16}S^{44}$, $_{18}Ar^{44}$, $_{20}Ca^{44}$, and $_{22}Ti^{44}$ which have near identical or identical experimental deformation parameter values. The core-polarization effects and model space were adopted through the inclusion of effective charges. The theoretical transition rate $B(E2)$, theoretical deformation parameters, and theoretical intrinsic quadrupole moments were calculated using two different interactions for each case, including *hasp* for the shell, *fpd6* for the shell, and *vpnp* for the *sd* shell, *kb3* for the *fp* shell, and through the use of different effective charges, namely the B-M, and ST effective charges, and the effective charges from NU-SH. The theoretical results for the transition rate, deformation parameter, and intrinsic quadrupole moment were found to be reasonably close to the experimental values when using, the *kb3*, and *vpnp* interactions, and B-M and ST effective charges, with the exception that the theoretical results determined for the $_{20}$Ca transition rate, deformation parameter and intrinsic quadrupole moment were underestimated comparing to the experimental values.

REFERENCES

1. A.H. Ali, M.T. Idrees. Study of deformation parameters (β2, δ) for ^{18,20,22,24,26,28}Ne isotopes in *sdpf*-shell. Karbala Int. J. Mod. Sci. 6(1) (2020) 11.
2. Y. Akiyama, A. Arima, T. Sebe. The structure of the *sd* shell nuclei: (IV). ^{20}Ne, ^{21}Ne, ^{22}Ne, ^{22}Na and ^{24}Mg. Nucl. Phys. A 138(2) (1969) 273.
3. R.A. Radhi, G.N. Flaiyh, E.M. Raheem. Electric Quadrupole Transitions of Some Even-Even Neon Isotopes. Iraqi J. Sci. 56(2A) (2015) 1047.
4. A.H. Ali. Shell Model for Study Quadrupole Transition Rates in B_2 in Some Neon Isotopes in *sd*-shell with Using Different Interactions. J. Astrophys. Aerospace Technol. 6(1) (2018) 160.

5. H. Hasper. Large scale shell-model calculations in the upper part of the sd shell: General description and energy levels for A = 36 - 39. Phys. Rev. C 19 (1979) 1482.
6. T.T.S. Kuo, G.E. Brown. Reaction matrix elements for the 0f-1p shell nuclei. Nucl. Phys. A 114(2) (1968) 241.
7. M. Hjorth-Jensen, T.T.S. Kuo, E. Osnes. Realistic effective interactions for nuclear systems. Phys. Rep. 261(3-4) (1995) 125.
8. J.B. McGrory, B.H. Wildenthal, E.C. Halbert. Shell-Model Structure of $^{42-50}$Ca. Phys. Rev. C 2 (1970) 186.
9. W.A. Richter et al. New effective interactions for the $0f1_p$ shell. Nucl. Phys. A 523(2) (1991) 325.
10. A. Poves, A. Zuker. Theoretical spectroscopy and the fp shell. Phys. Rep. 70(4) (1981) 235.
11. A.H. Ali, S.O. Hassoon, H. Tafash. Calculations of Quadrupole Deformation Parameters for Nuclei in *fp* shell. J. Phys.: Conf. Ser. 1178 (2019) 012010.
12. A. Novoselsky, M. Vallières, O. La'adan. Full *f-p* Shell Calculation of ^{51}Ca and ^{51}Sc. Phys. Rev. Lett. 79 (1997) 4341.
13. B.A. Brown, W.D.M. Rae. The Shell-Model Code NuShellX@MSU. Nucl. Data Sheets 120 (2014) 115.
14. A.H. Ali. Study of the Electric Quadrupole Moments for some Scandium Isotopes Using Shell Model Calculations with Different Interactions. Baghdad Sci. J. 15(3) (2018) 0304.
15. A. Bohr, B.R. Mottelson. *Nuclear Structure.* Vol. II: Nuclear Deformations (New York, Benjamin, (1975).
16. R.A. Radhi, A.H. Ali. Microscopic calculations of effective charges and quadrupole transition rates in Si, S and Ar isotopes. Iraqi J. Sci. 57(3B) (2016) 1999.
17. S. Raman, C.W. Nestor (Jr.), P. Tikkanen. Transition probability from the ground to the first-excited 2^+ state of even–even nuclides. Atom. Data Nucl. Data 78(1) (2001) 1.
18. J. Margraf et al. Deformation dependence of low lying M1 strengths in even Nd isotopes. Phys. Rev. C 47 (1993) 1474.
19. C.J. Van Der Poel et al. High-spin states in ^{34}Cl. Nucl. Phys. A 373(1) (1982) 81.
20. B. Pritychenko et al. Tables of E2 transition probabilities from the first 2^+ states in even-even nuclei. Atom. Data Nucl. Data Tables 107 (2016) 1.
21. W.A. Richter, S. Mkhize, B.A. Brown. sd-shell observables for the USDA and USDB Hamiltonians. Phys. Rev. C 78(6) (2008) 064302.

А. Х. Алі[1,2,*]

[1] Медичний коледж, Університет Фаллуджі, Фаллуджа, Ірак
[2] Центр біотехнології та навколишнього середовища, Університет Фаллуджі, Анбар, Ірак

*Відповідальний автор: dr.ahmedphysics@uofallujah.edu.iq

ПОРІВНЯННЯ МІЖ ТЕОРЕТИЧНИМИ РЕЗУЛЬТАТАМИ ТА ЕКСПЕРИМЕНТАЛЬНИМИ ДАНИМИ ІМОВІРНОСТЕЙ ПЕРЕХОДУ *B*(*E*2), ПАРАМЕТРІВ ДЕФОРМАЦІЇ ТА ВНУТРІШНІМИ КВАДРУПОЛЬНИМИ МОМЕНТАМИ ДЛЯ РІЗНИХ ЯДЕР З МАСОВИМ ЧИСЛОМ A = 44

Проведено порівняння теоретичних результатів з експериментальними даними для різних ядер (парно-парних), які мають однакове масове число A = 44 і мають близькі значення експериментального параметра деформації, таких як $_{16}S^{44}$, $_{18}Ar^{44}$, $_{20}Ca^{44}$ і $_{22}Ti^{44}$. Ефекти поляризації ядра та модельний простір були прийняті шляхом включення ефективних зарядів. Імовірності переходу *B*(*E*2), теоретичні параметри деформації та внутрішні квадрупольні моменти було розраховано з використанням двох різних взаємодій для кожного випадку; перший випадок – *hasp* взаємодія для ядер в *sd* оболонці та *fpd6* взаємодія для ядер в *fp* оболонці; у другому випадку – взаємодія *vpnp* для ядер у оболонці *sd* та взаємодія *kb3* для ядер у оболонці *fp*, також адаптовані до різних ефективних зарядів, таких як ефективні заряди Бора та Моттельсона, стандартні ефективні заряди та ефективні заряди від програми NuShellX. Теоретичні результати ймовірностей переходу *B*(*E*2), параметрів деформації і внутрішніх квадрупольних моментів виявилися близькими до експериментальних значень для цих ядер.

Ключові слова: порівняння, параметр деформації, ефективні заряди, ядра, внутрішні квадрупольні моменти.

Надійшла/Received 22.05.2023